JOURNAL OF PROPULSION AND POWER
Vol. 12, No. 6, November–December 1996

Transverse Gas Jet Injection Behind a Rearward-Facing Step

A. R. Karagozian,* K. C. Wang,† A.-T. Le,‡ and O. I. Smith§
University of California, Los Angeles, California 90095-1597

An experimental and theoretical study of the behavior of a transverse gas jet injected behind a rearward-facing step in supersonic flow is described. In-flight iodine planar laser-induced fluorescence imaging was performed to study this flowfield at NASA Dryden Flight Research Center using a flight test fixture situated under the fuselage of an F-104G aircraft. Jet structure and penetration data were obtained, in addition to limited characteristics for jet mixing and for supersonic flow over a rearward-facing step in a flow regime and for injection locations not extensively studied in the past. A model for jet behavior is described that places emphasis on the dynamics of the vortical structures observed to dominate jet cross section. The complex flowfield formed downstream of the step is represented by a combination of empirical and analytical correlations. Model predictions for jet trajectories compare reasonably well with results from the present in-flight experiments as well as with prior wind-tunnel experimental data.

Nomenclature

d = jet diameter
M_{ang} = Mach number beyond expansion fan
M_j = jet Mach number
M_{rec} = Mach number in recirculation region
M_∞ = freestream Mach number
p_{ang} = static pressure beyond expansion fan
p_b = static pressure surrounding jet at injection location
p_j = static pressure of jet at injection
p_{rec} = static pressure in recirculation region
p_{refl} = static pressure downstream of reflected shock
p_6 = static pressure measured at transducer location, Fig. 3
p_∞ = freestream static pressure
R = jet-to-crossflow momentum flux ratio
U_j = velocity of jet at injection
U_∞ = freestream velocity
X_{reat} = distance between step and reattachment location
X_{st} = distance from center of jet exit to step
x = distance downstream of center of jet exit
Z_{st} = step height
z = distance from injection wall
ε = shear-layer growth angle
θ = angle of turning through expansion fan
ρ_j = jet density at injection
ρ_∞ = freestream gas density

Introduction

TRANSVERSE fuel injection behind a rearward-facing step is a flow configuration that has been suggested as a means of enhancing mixing and combustion completeness in scramjet and other high-speed aircraft engines.[1] For the case of supersonic upstream flow, injecting fuel transversely behind a rearward-facing step enables the jet to penetrate well into the (locally low-speed) flow before being turned by supersonic crossflow. Enhanced transverse jet penetration has been associated with enhanced mixing[1–5] because of the nature of the streamwise vorticity associated with the jet cross section.[6] Recent experimental studies of this flowfield have been undertaken using planar laser-induced fluorescence (PLIF) visualization techniques for both nonreacting[4,8] and reacting[3,5,7] jets in air. Full-scale numerical simulations of this flowfield have also been conducted.[9,10] Combustion experiments for this mode of fuel injection indicate that the configuration gives relatively rapid autoignition and flame holding at low total temperatures,[3,5,11] and that mixing may be enhanced by either reducing the freestream stagnation temperature[3,5] or by seeding the jet with a higher density gas,[7] effectively increasing jet momentum.

A gas jet injected transversely behind a rearward-facing step in supersonic flow potentially encounters several distinct, complex regions of flow. Figure 1 describes the current understanding of these flow regions,[12] each of which can be characterized by the Mach number, static pressure, and flow direction in that region. As indicated in the figure, the supersonic flow first passes through an expansion fan (two dimensional in the region of present investigation), which forms at the step. Beyond the relatively uniform supersonic flow in the region past the fan (labeled with flow conditions M_{ang} and p_{ang}), a shear layer forms, across which the flow transitions from supersonic to subsonic in the low-speed, recirculating flow regime. The av-

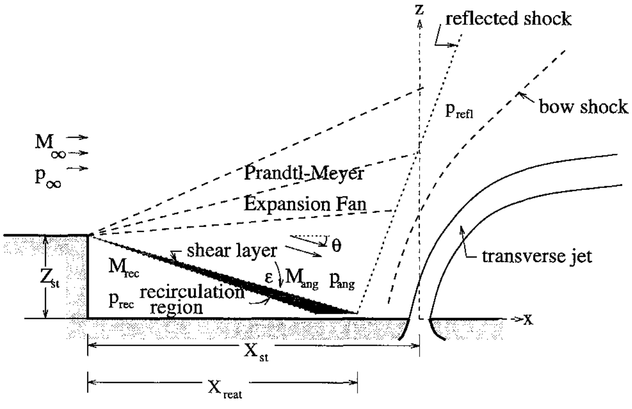

Fig. 1 Schematic of flow regions associated with transverse jet injection behind a rearward-facing step in supersonic crossflow. Injection location shown is beyond the reattachment point, for clarity.

Received Oct. 21, 1995; revision received April 8, 1996; accepted for publication April 16, 1996.

*Professor, Department of Mechanical and Aerospace Engineering. Associate Fellow AIAA.

†Graduate Student Researcher; currently Engineer, SPARTA, Inc., NASA Dryden Flight Research Center, Edwards, CA 93523. Member AIAA.

‡Graduate Student Researcher.

§Professor, Department of Mechanical and Aerospace Engineering.

erage pressure in the recirculation cell p_{rec} has been found experimentally[12–18] to be roughly equal to the pressure in the angled uniform flow regime p_{ang}. The shear layer reflects from the wall (at an effective reattachment location X_{reat} from the step) as an oblique shock wave. While the reattachment point and turning angle θ are dependent on upstream Mach number, they are largely independent of wall geometry or downstream disturbances.[16,18] It is into this complex flowfield that the gas jet is transversely injected. The jet injection location shown in Fig. 1 is for the case where injection occurs beyond the reattachment point and reflected shock location. This is drawn for clarity; in the present set of experiments, injection actually occurs at two different locations that are determined to be within the recirculation region.

The present study describes recent flight test experiments conducted for nonreacting, transverse gas jet injection downstream of a rearward-facing step in supersonic flow using PLIF imaging of iodine seeded in the jet. Flow conditions and injection locations that have not been extensively explored are examined here: the jets are somewhat underexpanded, with freestream Mach numbers that lie between 1.4–1.8 and with jet injection locations that lie at one and four step heights downstream of the step. Prior wind-tunnel studies have examined single nonreacting jet injection located at three[7] and four[8] step heights downstream, in addition to staged injection at three step heights.[4] The present flight experiments illuminate the fundamental structure of the transverse jet while removing the effects of wall confinement that are present in wind-tunnel experiments. In addition, the present work describes a relatively simple, computationally inexpensive model for this flowfield whose predictions may be compared with present flight data as well as with wind-tunnel data.[8] Reasonable comparisons indicate that the model could be useful as a design tool in optimizing transverse jet penetration.

In-Flight Experiments

In cooperation with the NASA Dryden Flight Research Center at Edwards Air Force Base in California, the F-104G research aircraft no. 826 was utilized as a flying wind-tunnel platform for the present transverse jet experiments. This Lockheed F-104G was modified during the 1960s to carry a low AR fin on the underside of the fuselage for the purpose of conducting flight testing. This flight test fixture (FTF) has evolved into a highly versatile facility for fluid mechanics research.[19]

The F-104G was used in the present study to conduct experiments on transverse gas jets injected normally into uniform transonic crossflows as well as into supersonic flows past a rearward-facing step. Results from the uniform crossflow experiments are described in Ref. 20 and are compared with predictions of jet behavior obtained from recent modeling efforts.[21–23] A brief description of the flight test experiments follows; further details on the flight apparatus and testing may be found in Refs. 20 and 24.

Flight Test Fixture

The experimental flight test apparatus was composed of three subsystems: 1) one containing the laser and its associated optics, 2) one containing the intensified camera and its filters and mirrors responsible for imaging the fluorescent jet, and 3) a jet formation subsystem that included all components involved in the storage, pressure regulation, heating, and flow control of the nitrogen gas and iodine seed. A photograph of the FTF appears in Fig. 2.

PLIF imaging of an iodine-seeded nitrogen jet was used in these flight tests to visualize the transverse jet flowfield. A sheet of laser light from a pulsed diode pumped Nd:YAG laser at 532.25 nm was used to illuminate a streamwise planar cross section of the jet. The jet emanated from the side of the FTF. The laser sheet was formed in flight by means of a −6.35-mm focal length front surface cylindrical mirror that expanded the beam perpendicularly to the FTF in the streamwise direction. A high-reflectivity mirror housed in the optical canopy acted as a turning mirror, positioning the light sheet on the plane of the jet. This positioning was dependent on the aircraft's angle of attack (AOA) (approximately +3 deg alpha for the F-104G in level flight); provision for adjustment was made via a multiaxis kinematic mirror mount. A 300-mm-fm cylindrical lens at the front of the canopy acted to thin the sheet.

Flowfield images were captured by a high-speed gated intensified video camera synchronized to the laser pulse rate and equipped with appropriate optical filters to improve the signal-to-noise ratio. An ITT image-intensified solid-state charge-coupled device (CCD) camera (F4577) was used, incorporating a Generation II image intensifier, an 11-mm CCD sensor, and integrated electronics to produce a very high-resolution RS-170 video signal. The image intensifier used a microchannel plate (MCP) current amplifier with an S20 photocathode. The CCD was a Texas Instruments TC241 488(V) × 754(H) pixel, frame-transfer device with a 6.6 × 8.8 mm image format. The electronics provided photocathode gating, gain control, and an automatic iris control signal. The F4577 used a tapered fiber optic coupling between the intensifier and CCD to achieve high-efficiency image transfer. Background light was rejected using an Oriel high-pass interference filter with a 530 nm cut-on.

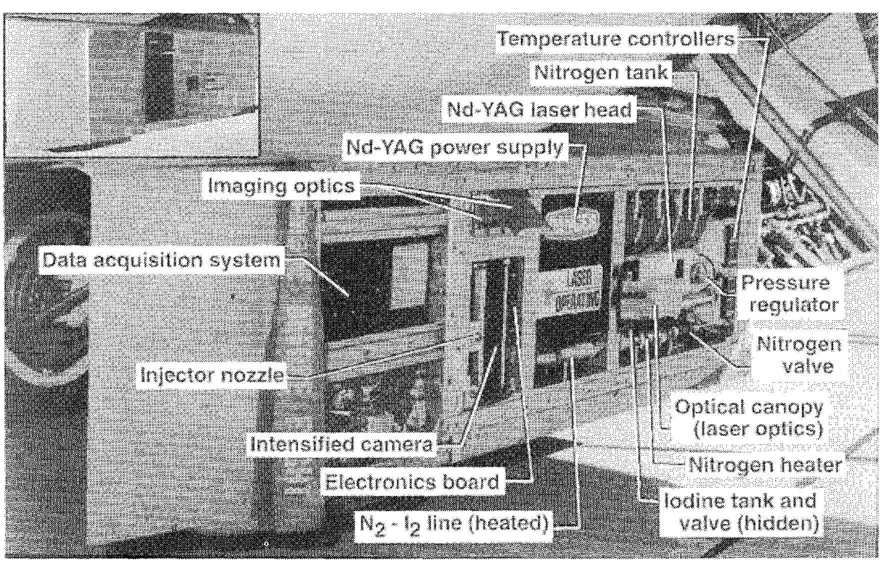

Fig. 2 Photograph of internal components of flight test fixture. Flight test fixture with cover appears in upper left corner.

Iodine fluorescence in the jet was imaged onto the intensifier focal plane using a system of one internal and one external mirror, along with a standard Nikon 28-mm f2.8 camera lens on the F4577. The internal mirror was oriented at a 45-deg angle and mounted just above the camera lens, allowing an outward view. This arrangement resulted in a viewable area of about 11.5 × 16.6 cm in the plane of the jet. The framing rate of the camera was 30 Hz.

Nitrogen for jet formation was stored at pressures up to 3000 psig in a 5.1-l high-pressure cylinder. The jet was only operated when the experiment reached a desired flight test condition, at which time a solenoid valve was activated for a preprogrammed duration (variable from 6 to 13 s). This time period allowed for virtually steady-state jet behavior to be achieved, as verified later from PLIF images. Iodine vapor was seeded into the main nitrogen flow at a tee-branch in concentrations of at least 2000 ppm; seeding rates were regulated by controlling the temperature, and thus the pressure, of the iodine reservoir/cell. Uncertainties in iodine concentrations were of the order 200 ppm.

After seeding, the N_2–I_2 mixture was carried in heated stainless steel lines and finally passed through a sonic nozzle that injected the gas into the flowfield downstream of a rearward-facing step. The nozzle exit diameter was 7.2 mm and the step height was three times the exit diameter, 21.6 mm. Injection locations examined here were at one and four step heights downstream of the step. The width of the step was approximately 30.5 cm, sufficiently wide to ensure that end effects would not influence jet behavior. It is noted that, in the absence of an opposite wall, the jet diameter can be made considerably larger than in wind-tunnel tests.[7,8]

Upon reaching a desired flight test condition, the pilot fired the experiment, then stabilized the flight Mach number, altitude, and AOA as best as possible for the duration of the experiment. The entire experiment was operated solely by the pilot in flight. Images of the illuminated jet were viewed in real time during the flights as well as recorded on VHS and Beta tape formats for postflight review.

Flow Conditions

The present flowfield may be characterized by geometrical factors (X_{st} and Z_{st}) and by flow features (jet and crossflow characteristics). As shown in Fig. 1, X_{st} takes on negative values in the present orientation since the origin was situated at the center of the injector nozzle. This distance is given in terms of the height of the step Z_{st}.

The overall jet-to-crossflow momentum flux ratio for a transverse jet is typically defined by

$$R = \frac{\gamma_j p_j M_j^2}{\gamma_\infty p_\infty M_\infty^2}$$

Fundamental incompressible transverse jet behavior, e.g., trajectory shape, spreading, and mixing, is typically dependent most strongly on the momentum flux ratio.[6,25] For the compressible jet in compressible crossflow, R still plays a dominant role,[8] but the jet is also affected separately by Mach numbers and pressures, especially if the jet is highly underexpanded.[2,7,26] In the case where the jet is injected transversely behind a rearward-facing step, the more relevant flow conditions are perhaps those associated with the jet and local conditions into which injection occurs.

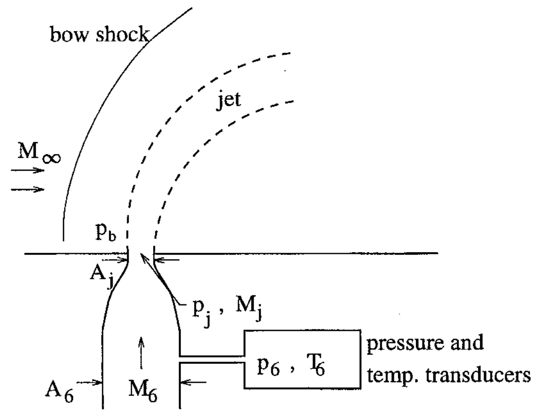

Fig. 3 Schematic diagram of pertinent flow properties in the vicinity of the jet nozzle exit.

From flight test data, the jet, freestream, and surrounding flow conditions were evaluated as follows, with reference to the nozzle schematic shown in Fig. 3. The pressures p_b (surrounding the jet, behind a bow shock, if present) and p_6 (at a pressure transducer upstream of the converging section) were measured in flight. The nozzle exit was situated at a local area minimum, and isentropic flow was assumed in the nozzle. The freestream Mach number M_∞ was measured using a pitot probe situated in the noseboom of the F-104G, and the static temperature of the freestream was determined using a total temperature probe on the F-104G radome. Prior flight test data[19] were incorporated to account for downwash, body, and shock wave effects.

Clearly, if $p_b/p_6 \leq 0.528$, the nozzle is choked and p_j may be evaluated from the known area ratio A_6/A_j and p_6. This situation was observed for all injection conditions in the present experiments, verifying that jet injection occurred at sonic conditions. Errors did arise in p_j because of data/measurement scatter (6–12%), yielding error bounds believed to be of the order 7–13% in the estimate for R and of the order 1% in M_j. Errors in crossflow conditions were of the order 2% for M_∞.

The estimated location of jet injection with respect to the flow regimes shown in Fig. 1 was determined as follows. Assuming initially that injection occurred within the recirculation zone, $p_b = p_{rec}$, which was assumed to be equal to p_{ang}, consistent with Refs. 12–18. p_{ang}/p_∞ is a function of M_∞ and M_{ang} assuming isentropic flow through the expansion fan, an approximation largely consistent with the observations of Refs. 12 and 17. The angle of turning by the fan θ may then be determined; this also estimated the location of reattachment X_{reat}. These assumptions and approach are clearly appropriate for injection at one step height downstream of the step (cases a and c) since prior experiments[8,12,16,17] indicate turning angles of 15 deg or higher for upstream Mach numbers of 2 or higher. For injection at four step heights downstream of the step (case b), a verification that injection occurs within the recirculation zone was necessary. This was accomplished by estimating the turning angle for this case by linear interpolation of turning angles found in cases a and c; the reflected shock angle and its downstream pressure p_{refl} could then be determined. The pressure that would be seen by the jet at this ignition location was computed to be much higher than that actually measured p_b. Hence, the injection regime for case b was ulti-

Table 1 Flow conditions for in-flight experiments

Case	M_∞	M_j	U_j/U_∞	p_j/p_∞	p_j/p_b	R	X_{st}	X_{reat}[a]	θ,[a] deg
a	1.42	1.0	0.886	1.465	1.97	0.726	$-Z_{st}$	$-9.5Z_{st}$	6
b	1.55	1.0	0.811	1.748	3.00	0.726	$-4Z_{st}$	$-5.5Z_{st}$	10.3
c	1.77	1.0	0.701	1.544	3.11	0.485	$-Z_{st}$	$-4.6Z_{st}$	12.3

[a]Estimate.

mately computed as done for cases a and c, yielding the set of flow parameters shown in Table 1. As indicated, the injection location for case b did lie somewhat upstream of the reattachment point. It should be noted that, for all cases considered here, the jets were underexpanded.

Model Description

The present effort made use of a previously described model for the behavior of a gas jet in supersonic, uniform crossflow,[21] a model that places emphasis on the dynamics of the compressible vortex pair structure observed to dominate the transverse jet cross section[2,6,8] and affect jet trajectory. A few minor modifications to the model were made by Le[23] to improve its numerical accuracy and theoretical consistency, as well as to prepare the model to accommodate the nonuniformity of upstream conditions associated with flow behind a step. These modifications include 1) for supersonic flow about the jet cross section, use of updated equivalent pressures, densities, and Mach numbers of the gas downstream of the bow shock based on output from a compressible vortex pair computation[27] and 2) an assumption that, before entrainment of crossflow occurs and the jet is expanded to the local pressure of the external flow, the mass flux across each cross-sectional jet slice is constant. Comparisons between the trajectories predicted by the modified transverse jet model[23] for uniform crossflow and those predicted by the original model[21] indicated a slight improvement with these refinements. While the model does not take into account the formation of a Mach disk within the jet, and thus is most appropriate for application to perfectly expanded or slightly underexpanded jets, it has been shown to be accurate to within 15% for pressure ratios p_j/p_b up to five,[21] and hence, should be appropriate in the present study.

As noted, a gas jet injected transversely behind a rearward-facing step in supersonic flow potentially encounters several distinct, complex regions of flow. To preserve the relative simplicity and computational efficiency of the present model, these data were extracted from present as well as prior experiments,[12–16,18] in addition to numerical data[28,29] and correlations using the method of characteristics. The methodology is described later.

In the present set of experiments, jet injection was determined to occur within the recirculation region, and hence, the average pressure in this region $p_{\rm rec}$ was known from direct measurement. Assuming $p_{\rm rec} = p_{\rm ang}$ across the shear layer, consistent with a number of supersonic shear-layer studies,[12–18] the Mach number and angle of turning in the angled flow region were determined. In general, if the recirculation zone pressure or other local conditions are not known a priori, some information with respect to the angle of turning must be provided as done in Ref. 12, for example.

Further conditions in the recirculation region were approximated by curve-fitting limited experimental and numerical data. One important feature of the transverse jet code[21] to be satisfied was that the flow encountered by the jet must be oriented positively in the x direction. Hence, it became necessary to assume uniform, low-speed subsonic flow in the recirculation region. Mach number and velocity in this region were curve fit from available data,[13,28,29] but the assumption of uniform subsonic flow in the positive downstream direction is an obvious limitation of the model.

The flow within the shear layer was approximated using a hyperbolic tangent approximation, consistent with experimental observations,[14] where ε is estimated as 0.0368. Finally, the flow beyond the reflected shock was determined in two stages: 1) as uniform flow through an oblique, straight shock before the shock encounters the expansion fan and 2) using the computed flow direction within the expansion fan, so that the local reflected shock angle and downstream conditions were solved by iteration using oblique shock relations.

In contrast to jet injection into a uniform crossflow, injection behind a step introduces a clear sensitivity to the location of jet introduction. It has not been conclusively established what effect transverse injection has on the surrounding flow, although recent wind-tunnel measurements[5] show that, even when the jet reacts with the crossflow, the freestream pressure is unaffected by combustion downstream of the step. As a consequence, the step is generally regarded to isolate the upstream flow from the jet and recirculation regions. The present calculation thus assumed that the jet did not influence the local flow upstream, except to the extent that a bow shock formed if the local crossflow became supersonic. The computational approach for shock capturing, using the method of Godunov,[30] is described in Ref. 21. Hence, at each step in flow time, the conditions upstream of the jet cross section were determined from the previous crossflow data, the flow's influence on the jet cross section (vortex pair separation, etc.) was then computed, and the trajectory of the vortex structure associated with the jet, for example, was determined.

Results

Four individual flight tests (takeoffs and landings) were successfully performed at NASA Dryden in January of 1994. Two of the flights, numbered 1410 and 1411, were for gas jets injected into uniform crossflow.[20] The other two flights, 1412 and 1415, contained test data for the jet injected downstream of a rearward-facing step, the case of present interest.

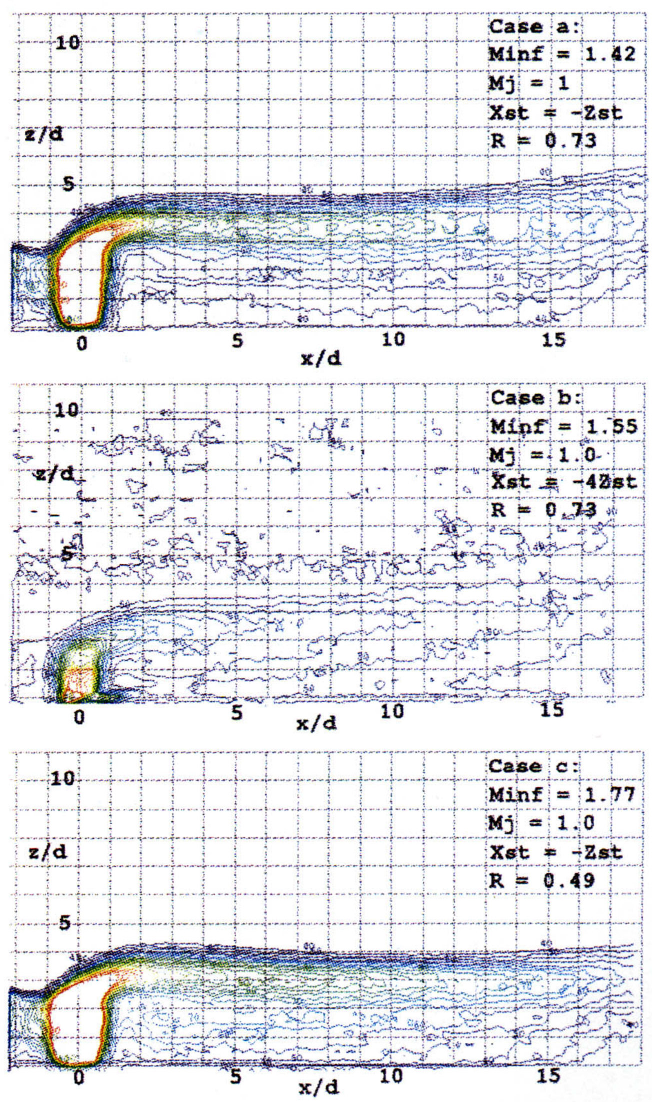

Fig. 4 Iodine concentration contours for flow conditions corresponding to flight cases a, b, and c listed in Table 1. Each grid marking shown represents one jet diameter.

Iodine PLIF images for the jet in crossflow were obtained for the duration of all experimental conditions described in Table 1. Approximate iodine concentration contours were produced by averaging iodine PLIF images over 135 frames, representing the latter 75% of the duration of jet injection, and then analyzing the images. The nozzle temperature varied over the initial 25% of the jet injection period, hence these images were not included in the averaging. The latter 75% of the jet injection period produced very stable transverse jets. It should be noted that, because of the undetermined temperature distributions and dilution of iodine within the jet, the possibility of variation in the Boltzmann fraction and collisional quenching renders the iodine fluorescence a more qualitative than quantitative representation of iodine concentration.

Approximate fluorescence/concentration contour plots for iodine are shown in Fig. 4 for the three cases run, noting from

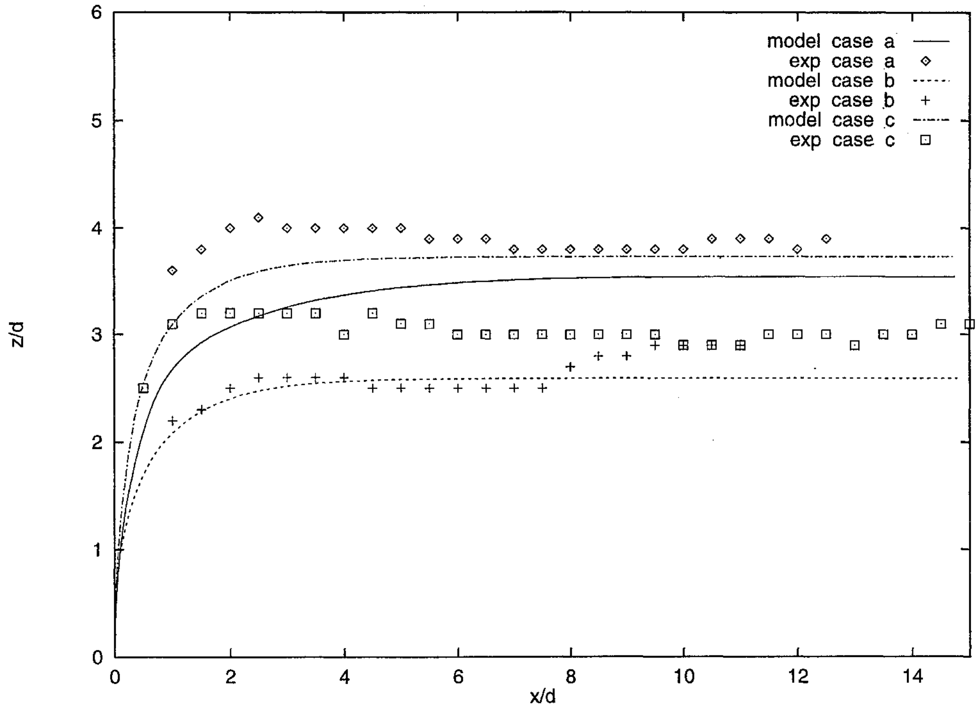

Fig. 5 Comparisons of loci of iodine concentration maxima from present flight experiments with vortex pair trajectories predicted by the present model. Test conditions correspond to those given in Table 1 for cases a, b, and c.

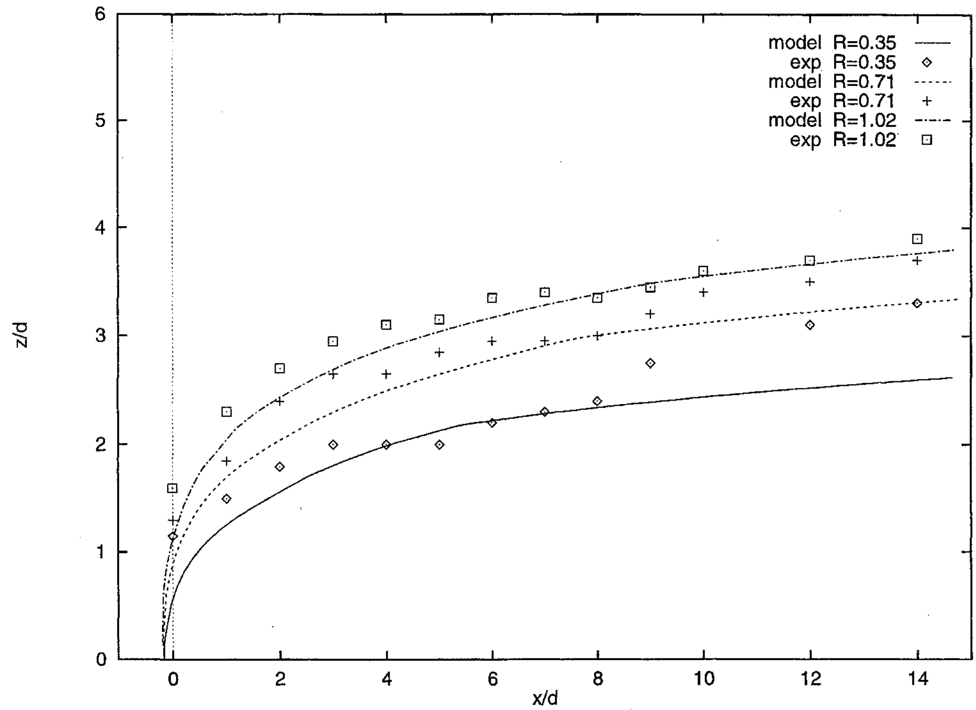

Fig. 6 Comparison of predicted trajectories of the tops of jets injected at a location $X_{st} = -4Z_{st}$ with experimental data,[8] for $M_\infty = 2.07$, $M_j = 1.0$, $U_j/U_\infty = 0.6$, and $\theta = 15.5$ deg.

the previous discussion that, while the quantitative interpretation of iodine concentrations may be approximate, the quantitative interpretation of overall jet structure and penetration beyond the step shear layer is very accurate except just downstream of the step in cases a and c, where optical scattering of the laser sheet from the step affects the iodine fluorescence signal. In general, the temperature field is symmetric across the jet cross section, and hence the loci of points of maximum fluorescence and iodine concentration should be the same. Color maps are consistent among the three plots. Highest concentrations of iodine are apparent in red, in the near-field potential core region of the jet, which extends vertically until the jet encounters the shear layer formed by the supersonic crossflow over the rearward step. The enhanced total jet penetration with injection further within the recirculation zone and with increased momentum flux ratio is evident in these images. Although injection for all three cases occurs within the recirculation region, case b is barely within this region, and the jet in this case is turned more quickly by the supersonic crossflow than in cases a and c.

The contours in Fig. 4 may also be used to compare the degree of mixing of jet and surrounding fluid for the three cases tested. Cases a and c each have injection at one step height downstream of the step, but case a has the higher momentum flux ratio and lower crossflow Mach number and, not surprisingly, exhibits greater penetration. Case a also exhibits

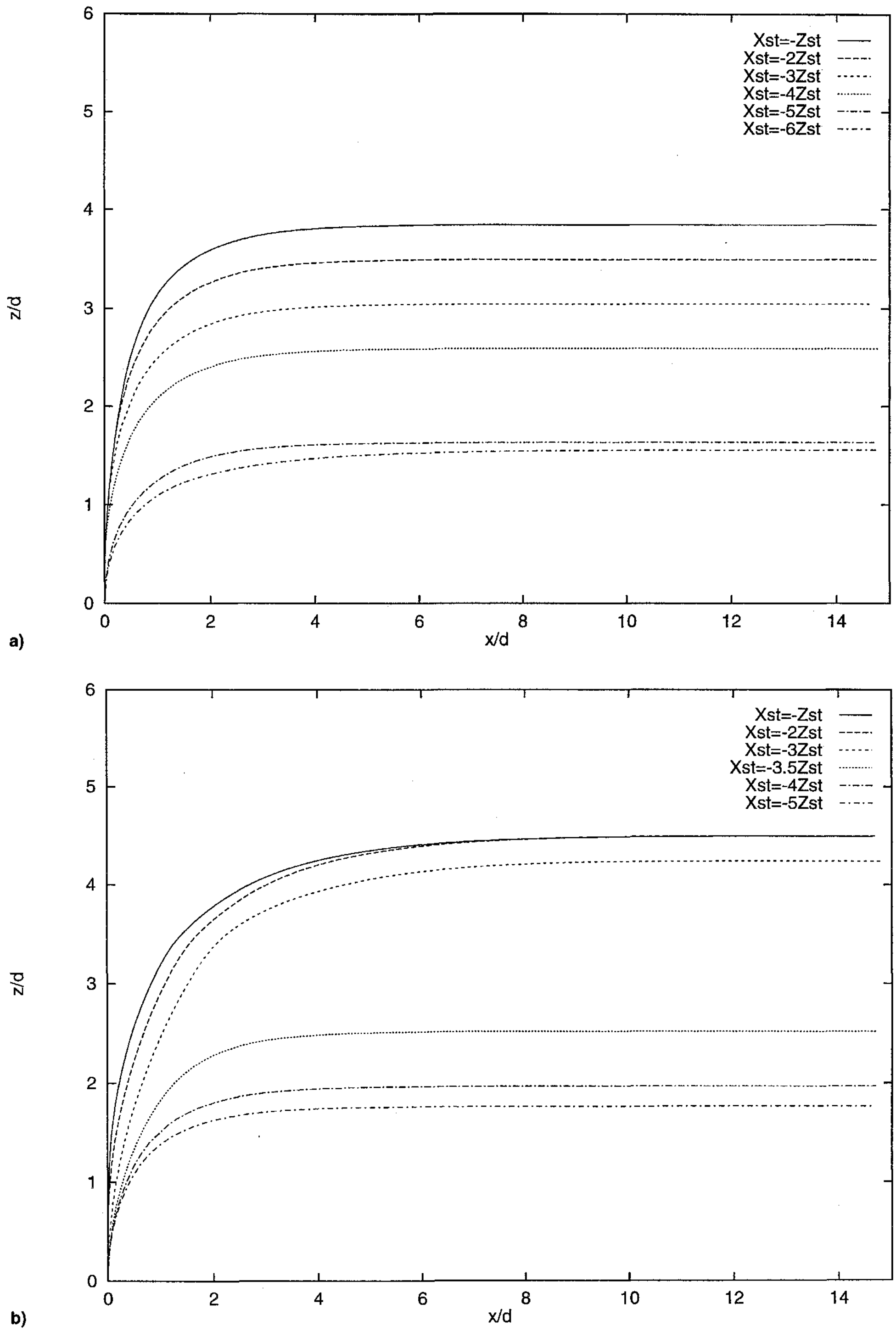

Fig. 7 Predicted centerline trajectories of jets injected at various positions behind a step: a) for $M_\infty = 1.55$, $M_j = 1.0$, $U_j/U_\infty = 0.81$, and $\theta = 10.3$ deg; and b) for $M_\infty = 2.07$, $M_j = 1.0$, $U_j/U_\infty = 0.6$, and $\theta = 15$ deg.

somewhat greater mixing (i.e., a more rapid reduction in iodine fluorescence along the trajectory) than does case c. This result confirms prior observations concerning the enhancement of mixing with greater momentum flux ratio and with greater jet penetration.[1-3,5,7]

Cases a and b, on the other hand, each have the same overall momentum flux ratio R, yet case b has injection at four step heights downstream with a higher crossflow Mach number and, again not surprisingly, exhibits lower jet penetration. The rate of mixing along the trajectory for case b is substantially greater than for case a, however, exhibited by the sharp drop in iodine signal. Even the rate of mixing beyond the point where the jet penetrates the step's shear layer appears to be greater in case b (which has a higher crossflow Mach number), than in case a. Clearly, penetration alone cannot be used as a predictor of the degree of jet mixing, especially in the vicinity of a rearward step; in fact, extremely high rates of fuel–air mixing may actually not be desirable for scramjet applications. The very high rate of mixing in case b could render this condition inappropriate for autoignition because of the very high strain rates that are known to delay or prevent ignition. Reduced ignition delay (resulting from reduced local rates of strain), alternatively, is known to enhance combustor performance during nonpremixed supersonic combustion.[1]

The loci of iodine fluorescence/concentration maxima here roughly correspond to the trajectory of the vortex pair associated with the jet cross section, since most of the jet fluid becomes concentrated within a few diameters into the vortical structures. It is these estimated loci of concentration maxima that may be compared with the model's prediction of the trajectory of the vortex pair, although the concentration contours in Fig. 4 demonstrate that these loci are approximate. The comparisons of concentration maxima loci with model predictions are shown in Fig. 5. Results for case a, with jet injection well within the recirculation region, indicate that the model, like the experiments, predicts enhanced penetration compared with injection further downstream within the zone, but at the same momentum flux ratio (case b). The model underpredicts far-field penetration of the jet for case a by about 8% overall and overpredicts far-field penetration in case c by about 20% overall; these are likely because of inaccuracies in representing the complex flow in the recirculation zone behind the step, which is significant for this injection location. In contrast, case b with jet injection at four step heights downstream of the step shows model prediction to be closer to the experimental trajectory (overall, within 7%). Since the jet is now injected just inside the recirculation zone, it is exposed to only a small part of the zone and inaccuracies in the modeling there have a lesser effect. The slight dip in the experimental trajectory near $x/d = 6$ in case b may be inherent to the transverse jet structure for certain flow conditions, as this type of behavior was observed in flight test results[20] as well as wind-tunnel studies[8] for jets in uniform supersonic crossflow, and thus, is not an outcome of shock reflection in a wind tunnel. This change in structure may in fact be a confirmation of the observations of Hollo et al.,[4] that there is a transition from vortex-dominated mixing to small-scale turbulent mixing along the jet trajectory.

The present model for jet injection behind a rearward-facing step may also be compared with trajectories from iodine PLIF measurements in a supersonic wind tunnel.[8] In these experimental studies, the jet was injected into a Mach 2 freestream at four step heights downstream of the step, placing the jet slightly beyond the recirculation zone (with a measured turning angle of 15.5 deg), in the region behind the reflected shock. Figure 6 indicates that the predictions agree quite well with data for the trajectory of the top of the jets (defined in the experiments as the location at which iodine concentrations are reduced to 5% of maximum).

It is also possible to perform parametric studies using the present model to determine the effects of injection location and other flow parameters. In Figs. 7a and 7b, jet vortex pair trajectories are shown for Mach 1.55 and 2.07 freestream flows, respectively, with various injection locations that allow the injector to be situated within the recirculation zone or outside the recirculation zone, downstream of the reflected shock structure. Turning angles of 10.3 and 15 deg are used for $M_\infty = 1.55$ and 2.07, respectively, based on present and wind-tunnel measurements.[12] These results indicate that injection well within the recirculation zone can result in a significant increase in jet penetration over injection outside the recirculation zone. In fact, injection even somewhat outside the recirculation region ($X_{st} \approx -5Z_{st}$ in Fig. 7a) often results in penetration that is nearly the same as for injection into uniform crossflow. Additional calculations also reveal that the degree of influence of the recirculation zone increases for smaller momentum flux ratios.

Conclusions

In summary, the present flight experiments have explored the behavior of a gas jet injected transversely behind a rearward-facing step in supersonic crossflow, in a flow regime and for injection locations previously unexplored. Iodine PLIF data give quantitative results for jet penetration and qualitative estimates for jet mixing. Supersonic flow over the rearward step without jet injection is also characterized to a limited extent, through estimates of turning angle and reattachment length.

A simple model for jet behavior is found to agree reasonably well with experimental data taken in a wind tunnel[8] as well as with the present flight test experiments. Parametric studies reveal that jet injection well within the recirculation zone could increase jet penetration significantly over that of injection into a uniform flow, while injection outside this region results in relatively little improvement in jet penetration. Increased jet penetration may generally imply greater jet mixing and improved autoignition,[1-4] especially for injection at a fixed location as jet-to-crossflow momentum flux ratio is increased, yet the present experiments demonstrate that penetration alone cannot be used to predict the jet's rate of mixing with crossflow. In fact, very rapid fuel–air mixing may be undesirable for scramjet applications in that extremely high strain rates associated with rapid mixing may act to delay or prevent ignition altogether. It is clear that further controlled jet injection experiments are required, for a greater variety of compressible flow conditions, to be able to make conclusive statements concerning mixing enhancement and ignition associated with the transverse fuel jet in the vicinity of a rearward-facing step.

Acknowledgments

This work was supported by NASA Dryden Research Center Grant NCC 2-374. The authors would like to thank Reed Maxwell and B. J. Petersen of UCLA for their assistance in the calculations reported here, and Albion Bowers and Kenneth Iliff of NASA Dryden Flight Research Center for their technical assistance in the experiments.

References

[1]Northam, G. B., and Anderson, G. Y., "Supersonic Combustion Ramjet Research at Langley," AIAA Paper 86-0159, Jan. 1986.

[2]Schetz, J. A., and Billig, F. S., "Studies of Scramjet Flowfields," AIAA Paper 87-2161, July 1987.

[3]Abbitt, J. D., III, Segal, C., McDaniel, J. C., Krauss, R. H., and Whitehurst, R. B., "Experimental Supersonic Hydrogen Combustion Employing Staged Injection Behind a Rearward-Facing Step," *Journal of Propulsion and Power*, Vol. 9, No. 3, 1993, pp. 472–478.

[4]Hollo, S. D., McDaniel, J. C., and Hartfield, R. J., Jr., "Quantitative Investigation of Compressible Mixing: Staged Transverse Injection into Mach 2 Flow," *AIAA Journal*, Vol. 32, No. 3, 1994, pp. 528–534.

[5]Segal, C., McDaniel, J. C., Whitehurst, R. B., and Krauss, R. H., "Mixing and Chemical Kinetics Interactions in a Mach 2 Reacting Flow," *Journal of Propulsion and Power*, Vol. 11, No. 2, 1995, pp. 308–314.

[6]Kamotani, Y., and Greber, I., "Experiments on a Turbulent Jet in Cross Flow," *AIAA Journal*, Vol. 10, No. 11, 1972, pp. 1425–1429.

[7]McMillin, B. K., Seitzman, J. M., and Hanson, R. K., "Comparison of NO and OH Planar Fluorescence Temperature Measurements in Scramjet Model Flowfields," *AIAA Journal*, Vol. 32, No. 10, 1994, pp. 1945–1952.

[8]McDaniel, J. C., and Graves, J., Jr., "Laser-Induced-Fluorescence Visualization of Transverse Gaseous Injection in a Nonreacting Supersonic Combustor," *Journal of Propulsion and Power*, Vol. 4, No. 6, 1988, pp. 591–597.

[9]Rogers, R. C., and Weidner, E. H., "Numerical Predictions of Residence Times Behind a Rearward Facing Step with Transverse Injection," 20th JANNAF Combustion Meeting, U.S. Naval Postgraduate School, Monterey, CA, 1983.

[10]Uenishi, K., Rogers, R. C., and Northam, G. B., "Numerical Predictions of a Rearward-Facing-Step Flow in a Supersonic Combustor," *Journal of Propulsion and Power*, Vol. 5, No. 2, 1989, pp. 158–164.

[11]Northam, G. B., Trexler, C. A., and McClinton, C. R., "Flameholding Characteristics of a Swept-Strut H_2 Fuel-Injector for Scramjet Applications," 17th JANNAF Combustion Meeting, Hampton, VA, 1980.

[12]Fletcher, D. G., and McDaniel, J. C., "Laser-Induced Iodine Fluorescence Technique for Quantitative Measurement in a Nonreacting Supersonic Combustor," *AIAA Journal*, Vol. 27, No. 5, 1989, pp. 575–580.

[13]Donaldson, J. C., "An Experimental Study of the Region of Separated Flow Downstream of a 0.75 in. Rearward-Facing Step at Mach Numbers 2.5, 3.5, and 5.0," ARO Inc., Arnold Engineering and Development Center, Air Force Systems Command, AEDC-TR-69-141, 1969.

[14]Papamoschou, D., and Roshko, A., "Compressible Turbulent Shear Layer: An Experimental Study," *Journal of Fluid Mechanics*, Vol. 197, Dec. 1988, pp. 453–477.

[15]Hartfield, R. J., Jr., Hollo, S. D., and McDaniel, J. C., "Planar Measurement Technique for Compressible Flows Using Laser-Induced Iodine Fluorescence," *AIAA Journal*, Vol. 31, No. 3, 1993, pp. 483–490.

[16]Roshko, A., and Thomke, G. J., "Observations of Turbulent Reattachment Behind an Axisymmetric Downstream-Facing Step in Supersonic Flow," *AIAA Journal*, Vol. 4, No. 6, 1966, pp. 975–980.

[17]Scherberg, M. G., and Smith, H. E., "An Experimental Study of Supersonic Flow over a Rearward Facing Step," *AIAA Journal*, Vol. 5, No. 1, 1967, pp. 51–56.

[18]Samimy, M., Petrie, H. L., and Addy, A. L., "A Study of Compressible Turbulent Reattaching Free Shear Layers," *AIAA Journal*, Vol. 24, No. 2, 1986, pp. 261–270.

[19]Meyer, R. R., "A Unique Flight Test Facility: Description and Results," International Council of the Aeronautical Sciences, Paper 82-5.3.3, Aug. 1982.

[20]Wang, K. C., Smith, O. I., and Karagozian, A. R., "In-Flight Imaging of Transverse Gas Jets Injected into Subsonic and Supersonic Crossflows," *AIAA Journal*, Vol. 33, No. 12, 1995, pp. 2259–2263.

[21]Heister, S. D., and Karagozian, A. R., "Gaseous Jet in Supersonic Crossflow," *AIAA Journal*, Vol. 28, No. 5, 1990, pp. 819–827.

[22]Heister, S. D., and Karagozian, A. R., "Vortex Modeling of Gaseous Jets in a Compressible Crossflow," *Journal of Propulsion and Power*, Vol. 6, No. 1, 1990, pp. 85–92.

[23]Le, A.-T., "Transverse Gaseous Jet Injection Behind a Rearward-Facing Step into a Supersonic Crossflow," M.S. Thesis, Univ. of California, Los Angeles, CA, 1991.

[24]Wang, K. C., "In-Flight Imaging of Transverse Gas Jets Injected into Transonic and Supersonic Crossflows," M.S. Project, Univ. of California, Los Angeles, CA, 1993; also NASA CR-186031, Nov. 1994.

[25]LeGrives, E., "Mixing Process Induced by the Vorticity Associated with the Penetration of a Jet into a Crossflow," *Journal of Engineering for Power*, Vol. 100, July 1978, pp. 465–475.

[26]Spaid, F. W., and Zukoski, E. E., "Further Experiments Concerning Secondary Injection of Gases into a Supersonic Flow," *AIAA Journal*, Vol. 4, No. 12, 1966, pp. 2216–2218.

[27]Heister, S. D., McDonough, J. M., Karagozian, A. R., and Jenkins, D. W., "The Compressible Vortex Pair," *Journal of Fluid Mechanics*, Vol. 220, Nov. 1990, pp. 339–354.

[28]Lin, W. H., "Numerical Analysis of Scramjet Flows in a Dump Combustor," AIAA Paper 91-1676, 1991.

[29]Yang, A. S., Hsieh, W. H., and Kuo, K. K., "Theoretical Study of Supersonic Flow Separation over a Rearward Facing Step," AIAA Paper 91-2161, 1991.

[30]Godunov, S. K., Abrodin, A. V., and Prokopov, G. P., "A Computational Scheme for Two-Dimensional Non-Stationary Problems of Gas Dynamics and Calculation of the Flow from a Shock Wave Approaching a Steady State," *U.S.S.R. Computational Mathematics and Math Physics*, 1961, pp. 1187–1219.

Color reproductions courtesy of NASA Dryden Flight Research Center